J|A|C|S ARTICLES

Published on Web 12/29/2008

Switchable Electrode Controlled by Enzyme Logic Network System: Approaching Physiologically Regulated Bioelectronics

Marina Privman,[†,‡] Tsz Kin Tam,[†] Marcos Pita,[†] and Evgeny Katz*[,†]

Department of Chemistry and Biomolecular Science, and NanoBio Laboratory, Clarkson University, Potsdam, New York 13699-5810, and Empire State College, State University of New York, Post Office Box 940, Black River, New York 13612-0009

Received November 10, 2008; E-mail: ekatz@clarkson.edu

Abstract: The logic network composed of three enzymes (alcohol dehydrogenase, glucose dehydrogenase, and glucose oxidase) operating in concert as four concatenated logic gates (AND/OR), was designed to process four different chemical input signals (NADH, acetaldehyde, glucose, and oxygen). The cascade of biochemical reactions culminated in pH changes controlled by the pattern of the applied biochemical input signals. The "successful" set of inputs produced gluconic acid as the final product and yielded an acidic medium, lowering the pH of a solution from its initial value of pH 6−7 to the final value of ca. 4. The whole set of the input signal combinations included 16 variants resulting in different output signals. Those that corresponded to the logic output **1**, according to the Boolean logic encoded in the logic circuitry, resulted in the acidic medium. The pH changes produced in situ were coupled with a pH-sensitive polymer-brush-functionalized electrode, resulting in the interface switching from the OFF state, when the electrochemical reactions are inhibited, to the ON state, when the interface is electrochemically active. Soluble $[Fe(CN)_6]^{3-/4-}$ was used as an external redox probe to analyze the state of the interface and to follow the changes produced in situ by the enzyme logic network, depending on the pattern of the applied biochemical signals. The chemical signals processed by the enzyme logic system and transduced by the sensing interface were read out by electrochemical means (cyclic voltammetry and Faradaic impedance spectroscopy). This readout step features a "sigmoid" processing of the signals that provides "filtering" and significantly suppresses errors. Coupling between signal-processing enzyme logic networks and electronic transducers will allow future "smart" bioelectronic devices to respond to immediate physiological changes and provide autonomous signaling/actuation depending on the concentration patterns of the physiological markers.

Introduction

Chemical computing, a research subarea of unconventional computing,[1] usually aims at mimicking simple Boolean logic operations performed by chemical systems.[2] In most cases chemical logic operations are activated by external physical signals (e.g., light,[3] magnetic field,[4] or electrochemical potential[5]) and, sometimes, by chemical signals (e.g., pH changes or metal cations additions).[6] The output signals generated by the chemical logic systems are usually read by optical methods[7] (absorbance or fluorescence spectroscopy) or by electrochemical means[8] (currents or potentials generated on electrodes or field-effect transistors). Normally, the physical nature of the input and output signals is different, thus making the assembly of multicomponent logic networks difficult or impossible. Usually, the complexity of the chemical computing systems does not exceed a single Boolean logic operation, such as AND or OR. Complex multicomponent chemical logic systems usually require ingenious supramolecular ensembles to allow compatibility between processing information subunits.[9] Supramolecular systems operating as molecular machines were designed and

[†] Clarkson University.
[‡] Empire State College.

(1) (a) Teuscher, C., Adamatzky, A., Eds.; *Unconventional Computing 2005: From Cellular Automata to Wetware*; C. Luniver Press: Beckington, U.K., 2005. (b) Matsumaru, N.; Centler, F.; Di Fenizio, P. S.; Dittrich, P *Int. J.Unconventional Comput.* **2007**, *3*, 285–309.
(2) (a) De Silva, A. P.; Uchiyama, S. *Nat. Nanotechnol.* **2007**, *2*, 399–410. (b) Credi, A. *Angew. Chem., Int. Ed.* **2007**, *46*, 5472–5475.
(3) (a) Szacilowski, K.; Macyk, W.; Stochel, G. *J. Am. Chem. Soc.* **2006**, *128*, 4550–4551. (b) Katz, E.; Shipway, A.N. In *Bioelectronics: From Theory to Applications*; Willner, I., Katz, E., Eds.; Wiley−VCH: Weinheim, Germany, 2005; Chapt. 11, pp309−338. (c) Pischel, U.; Heller, B. *New J. Chem.* **2008**, *32*, 395–400.
(4) Vasilyev, S.; Pita, M.; Katz, E. *Electroanalysis* **2008**, *20*, 22–29.
(5) (a) Biancardo, M.; Bignozzi, C.; Hugh, D. C.; Redmond, G. *Chem. Commun.* **2005**, 3918–3920. (b) Zelikovich, L.; Libman, J.; Shanzer, A. *Nature* **1995**, *374*, 790–792. (c) Asakawa, M.; Ashton, P. R.; Balzani, V.; Credi, A.; Mattersteig, G.; Matthews, O. A.; Montalti, M.; Spencer, N.; Stoddart, J. F.; Venturi, M. *Chem.—Eur. J.* **1997**, *3*, 1992–1996.
(6) (a) Gunnlaugsson, T.; Mac Donail, D. A.; Parker, D. *Chem. Commun.* **2000**, 93–94. (b) Pina, F.; Roque, A.; Melo, M. J.; Maestri, I.; Belladelli, L.; Balzani, V. *Chem.—Eur. J.* **1998**, *4*, 1184–1191. (c) De Silva, P. A.; Gunaratne, N. H. Q.; McCoy, C. P. *Nature* **1993**, *364*, 42–44.
(7) (a) Magri, D. C.; Coen, G. D.; Boyd, R. L.; De Silva, A. P. *Anal. Chim. Acta* **2006**, *568*, 156–160. (b) Raymo, F. M.; Giordani, S. *Proc. Natl. Acad. U.S.A.* **2002**, *99*, 4941–4944.
(8) (a) Li, L.; Yu, M. X.; Li, F. Y.; Yi, T.; Huang, C. H. *Colloids Surf., A* **2007**, *304*, 49–53. (b) Wen, G. Y.; Yan, J.; Zhou, Y. C.; Zhang, D. Q.; Mao, L. Q.; Zhu, D. B. *Chem. Commun.* **2006**, 3016–3018. (c) Gupta, T.; Van der Boom, M. E. *Angew. Chem., Int. Ed.* **2008**, *47*, 5322–5326.

10.1021/ja8088108 CCC: $40.75

used to operate as chemical computing elements still performing rather simple functions despite their extreme synthetic complexity.[10]

Most of the problems hardly addressable by synthetic chemical systems can be solved easily and naturally by application of biomolecular systems. The recently emerged research field of biocomputing, based on application of biomolecular systems for processing chemical information, has achieved higher complexity of information processing while using much simpler chemical tools, due to the natural specificity and compatibility of biomolecular components.[11] Various Boolean logic operations were mimicked by enzyme systems,[12] allowing concerted operation of multienzyme assemblies performing simple arithmetic functions (half-adder/half-subtracter).[13] Although similar logic operations and arithmetic functions were also realized with nonbiological chemical systems,[14] the advantage of biomolecular systems was in the relative simplicity of various assembled logic schemes. The complexity of information-processing systems with enzymes could be easily scaled up, resulting in artificial biocomputing networks performing various logic functions (e.g., implication) and mimicking natural biochemical pathways.[15] Theoretical analysis of information processing by enzyme logic gates has predicted that at least 10 logic gates can be assembled in a sequence of logic operations before buildup of noise in the signal becomes a problem.[16]

Complexity of biomolecular computing systems, and particularly the speed of information processing, cannot compete with traditional silicon-based technology. However, biocomputing systems are not intended as substitutes for "normal" computers. Biocomputing systems could be used as interfaces between natural biochemical/physiological systems and artificial electronic devices or/and signal-responsive materials operating as chemical actuators. Biocomputing elements of even moderate complexity could allow effective interfacing between complex physiological processes and implantable biomedical devices, providing autonomous, individual, "upon-demand" medical care, which is the objective of the new nanomedicine concept.[17] Biocomputing also poses interesting theoretical challenges. On the conceptual level, it might help us understand how living organisms manage to control extremely complex and coupled biochemical reactions; that is, the hope is to cast biochemical (metabolic) pathways in the language of information theory.

Recently developed enzyme logic gates coupled with signal-responsive materials through pH changes generated in situ upon processing biochemical information were used to control biocatalytic electrodes,[18] Si chips,[19] biofuel cells,[20] and various nanostructured materials.[21] The present paper describes an application of a biocomputing logic system of scaled-up complexity to control electronic interfaces. We designed a multienzyme/multisignal-processing logic network modeling natural biological pathways and switching on a signal-responsive modified electrode upon application of the appropriate combinations of biochemical input signals. This is the first example of an artificial bioelectronic system where the electronic component is controlled by a biocomputing system of high complexity.

Experimental Section

Chemicals and Supplies. All chemicals were purchased and used as supplied without any further purification. From Sigma-Aldrich: β-nicotinamide adenine dinucleotide, reduced dipotassium salt (NADH), >95% purity; β-D-(+)-glucose, 99.5% GC; urea, ACS reagent 99−100%; glucose oxidase (GOx) type X-S from *Aspergillus niger* (EC 1.1.3.4); and alcohol dehydrogenase (ADH) from *Saccharomyces cervisiae* (EC 1.1.1.1). From Fluka: urease from jack beans (EC 3.5.1.5) and glucose dehydrogenase (GDH) from *Pseudomonas* sp. (EC 1.1.1.47). From T.J. Baker: sodium sulfate, anhydrous powder, 99%; and potassium ferricyanide, anhydrous, 99.8%. Potassium ferrocyanide, 98.5%, was from Fisher Scientific and acetaldehyde, technical grade, was from Eastman. Indium−tin oxide (ITO) coated conducting glass (20 ± 5 Ω/sq surface resistivity) from Aldrich served as the working electrode for electrochemical measurements. Prior to use, it was modified with a poly(4-vinyl pyridine) (P4VP) polymer brush, following a procedure that closely resembled the one described earlier.[22] It utilized P4VP from Sigma−Aldrich (molecular mass 160 kDa, $\rho = 1.101$ g·cm^{-3}); nitromethane, 96% from T.J. Baker; hydrogen peroxide, 30% solution, reagent, ACS from VWR International; ammonium hydroxide, ACS Plus from Fisher; bromomethyldimethylchlorosilane from Sigma−Aldrich; absolute ethanol from Pharmco; and HPLC-grade toluene from T.J. Baker. Water used in all experiments was ultrapure (18 MΩ·cm^{-1}), from NANOpure Diamond (Barnstead) source.

Electrode Modification. Commercially available indium−tin oxide (ITO) single-side coated glass slides were cut into 25 mm × 8 mm strips. These were sonicated for 15 min in ethanol and dried under a stream of argon. The procedure was repeated with methylene chloride. The initial cleaning steps were followed by immersing the strips for 1 h into a cleaning solution (heated to 60 °C in a water bath), composed of NH_4OH, H_2O_2, and H_2O in the ratio of 1:1:1 v/v/v (*Warning: This solution is highly reactive and extreme precautions must be taken upon its use*). Subsequently, the glass strips were rinsed several times with water, immersed for 20 min in water at room temperature, and then dried under argon. The freshly cleaned ITO strips were then immersed for 20 min into a 0.1% (v/v) solution of the silanization reagent, bromomethyldimethylchlorosilane, in toluene, at 70 °C. The silanized ITO was rinsed with several aliquots of toluene and dried under argon. Then 60 μL of the P4VP solution in nitromethane (10 mg·mL^{-1}) was

(9) (a) Margulies, D.; Felder, C. E.; Melman, G.; Shanzer, A. *J. Am. Chem. Soc.* **2007**, *129*, 347–354. (b) Qian, J. H.; Qian, X. H.; Xu, Y. F.; Zhang, S. Y. *Chem. Commun.* **2008**, 4141–4143.
(10) Flood, A. H.; Ramirez, R. J. A.; Deng, W. Q.; Muller, R. P.; Goddard, W. A.; Stoddart, J. F. *Aust. J. Chem.* **2004**, *57*, 301–322.
(11) (a) Shao, X. G.; Jiang, H. Y.; Cai, W. S. *Prog. Chem.* **2002**, *14*, 37–46. (b) Saghatelian, A.; Volcker, N. H.; Guckian, K. M.; Lin, V. S. Y.; Ghadiri, M. R. *J. Am. Chem. Soc.* **2003**, *125*, 346–347. (c) Ashkenasy, G.; Ghadiri, M. R. *J. Am. Chem. Soc.* **2004**, *126*, 11140–11141.
(12) (a) Strack, G.; Pita, M.; Ornatska, M.; Katz, E. *ChemBioChem* **2008**, *9*, 1260–1266. (b) Baron, R.; Lioubashevski, O.; Katz, E.; Niazov, T.; Willner, I *Org. Biomol. Chem.* **2006**, *4*, 989–991. (c) Baron, R.; Lioubashevski, O.; Katz, E.; Niazov, T.; Willner, I. *J. Phys. Chem. A* **2006**, *110*, 8548–8553.
(13) Baron, R.; Lioubashevski, O.; Katz, E.; Niazov, T.; Willner, I. *Angew. Chem., Int. Ed.* **2006**, *45*, 1572–1576.
(14) Pischel, U. *Angew. Chem., Int. Ed.* **2007**, *46*, 4026–4040.
(15) (a) Niazov, T.; Baron, R.; Katz, E.; Lioubashevski, O.; Willner, I. *Proc. Natl. Acad. Sci. U.S.A.* **2006**, *103*, 17160–17163. (b) Strack, G.; Ornatska, M.; Pita, M.; Katz, E. *J. Am. Chem. Soc.* **2008**, *130*, 4234–4235.
(16) Privman, V.; Strack, G.; Solenov, D.; Pita, M.; Katz, E. *J. Phys. Chem. B* **2008**, *112*, 11777–11784.
(17) (a) Seetharam, R. N. *Curr. Sci.* **2006**, *91*, 260. (b) Briquet-Laugier, V.; Ott, M. O. *Biofutur* **2006**, *265*, 57–62.
(18) Tam, T. K.; Zhou, J.; Pita, M.; Ornatska, M.; Minko, S.; Katz, E. *J. Am. Chem. Soc.* **2008**, *130*, 10888–10889.
(19) Krämer, M.; Pita, M.; Zhou, J.; Ornatska, M.; Poghossian, A.; Schöning, M.J.; Katz, E. *J. Phys. Chem. B* (in press).
(20) Amir, L.; Tam, T. K.; Pita, M.; Meijler, M. M.; Alfonta, L.; Katz, E. *J. Am. Chem. Soc.* (in press).
(21) (a) Pita, M.; Minko, S. Katz, E. *J. Mater. Sci.: Mater. Med.* **2008** (in press; ASAP article; DOI 10.1007/s10856-008-3579-y). (b) Motornov, M.; Zhou, J.; Pita, M.; Gopishetty, V.; Tokarev, I.; Katz, E.; Minko, S. *Nano Lett.* **2008**, *8*, 2993–2997.
(22) Tam, T. K.; Ornatska, M.; Pita, M.; Minko, S.; Katz, E. *J. Phys. Chem. C* **2008**, *112*, 8438–8445.

applied to the surface of each ITO glass strip, and the strips were left to react overnight in a vacuum oven at 140 °C. The final cleaning steps, to remove the unbound polymer, consisted of soaking for 10 min in ethanol, followed by an additional 10 min in a dilute solution of H_2SO_4 (pH 3). Modified electrodes were stored under water.

Composition of Enzyme Logic Solutions. All solutions were unbuffered, 0.1 M in Na_2SO_4, and contained the three enzymes that served as the "machinery" for the Boolean logic gates. The two concatenated AND gates, based on ADH (10 units·mL^{-1}) and GDH (10 units·mL^{-1}), were coupled with the third AND gate, based on GOx (10 units·mL^{-1}, unless specified otherwise). The concerted operation of GOx and GDH, both producing gluconic acid, resulted in the OR gate operation. The inputs used to activate the gate based on ADH were 0.5 mM NADH and 5 mM acetaldehyde. Its output, NAD^+ and 12.5 mM glucose, served as input for the gate based on GDH. Glucose, 12.5 mM, and dissolved oxygen in equilibrium with air served as inputs for the gate based on GOx. These concentrations corresponded to the Boolean input value of **1**. The absence of NADH, acetaldehyde, glucose, or oxygen corresponded to the respective Boolean input value of **0**. Deoxygenation (to produce O_2 input signal equal to logic **0**) was achieved by bubbling Ar through the working solution for 10 min prior to initiation of the biocatalytic reactions by adding deoxygenated NADH, acetaldehyde, and glucose as needed, while maintaining the system under the Ar blanket. Solutions used for electrochemical measurements also contained 10 mM $K_3Fe(CN)_6$ and 10 mM $K_4Fe(CN)_6$. The Boolean output signal **1** was acidic pH (pH < 4.3). Its in situ reset to the value of **0** (pH > 6) was achieved by adding urease (2.5 units·mL^{-1}) and urea (2.5 mM).

Measurements. The pH measurements were performed with Mettler Toledo SevenEasy pH-meter. Electrochemical measurements were carried out with an ECO Chemie Autolab PASTAT 10 electrochemical analyzer, using the GPES 4.9 (general purpose electrochemical system) software package for cyclic voltammetry and FRA 4.X (frequency response analyzer) for the Faradaic impedance measurements. All the measurements were performed at ambient temperature (23 ± 2 °C), in a standard three-electrode cell (ECO Chemie). The working electrode was a P4VP-modified ITO glass electrode with a geometrical area of 1.04 cm^2 (note that the typical surface roughness factor for ITO electrodes is ca. 1.6 ± 0.1).[23] A Metrohm Ag|AgCl|KCl, 3 M, electrode served as a reference electrode and a Metrohm Pt wire was used as a counter electrode. The Faradaic impedance spectra were recorded in the frequency range of 10 kHz−10 mHz, while a bias potential of 0.17 V and equilibration time of 5 s were applied. The values of electron transfer resistance, R_{et}, were derived from the recorded impedance spectra by use of the commercial software ZView, version 2.1b, Scribner Associates, Inc., by fitting the experimental data to the Randles−Ershler equivalent circuitry.[24] Cyclic voltammograms were recorded in the potential range from −0.15 to 0.6 V after an equilibration for 4 s at the starting potential. The potential scan rate was 100 mV·s^{-1}. Peak currents for each input combination were obtained from a second scan. In the experiments with variable concentrations of glucose, biocatalytic reactions at each concentration of glucose were carried out for 20 min prior to recording of cyclic voltammograms. To achieve a maximum reaction rate, air was bubbled through a solution for the first 10 min. Subsequently, working electrode was immersed into a solution and cyclic voltammograms were recorded after an additional 10 min.

Results and Discussion

Signal-responsive electrodes with chemically modified surfaces can switch interfacial electron transfer reactions ON and OFF upon application of various physical (e.g., light, magnetic field, applied potentials) and chemical (e.g., pH value) signals.[25] The mechanism of the switching process depends on the properties of the modified surface and applied signals. Recently, we developed modified electrodes functionalized with polyelectrolyte polymer brushes that reversibly change from a shrunken to a swollen state and back, in response to changes in pH values.[26] The electrode surface was effectively blocked for communicating with an external soluble redox probe when the polymer brush was in the shrunken state, resulting in a hydrophobic surface. Upon swelling of the polymer brush, the electrode surface became exposed to the solution and electrochemically active. Transitions between the shrunken and swollen states can be controlled by changing the solution pH, yielding the swollen, open state of the interface upon protonation of the polyelectrolyte chains at acidic conditions (pH < pK_a of the polyelectrolyte). Deprotonation of the polyelectrolyte (pH > pK_a) resulted in the shrunken state of the polymer brush, switching OFF the interfacial electron-transfer processes because of inaccessibility of the electrode surface for an external redox probe (Scheme 1). A detailed study of the switchable properties of the polymer-brush-modified electrodes was published elsewhere.[26] A similar approach was also applied to switch ON and OFF the electrochemical properties of a polymer-brush layer loaded with redox species.[18,22]

In the present study, we used a P4VP-functionalized ITO electrode that demonstrated the swollen hydrophilic interface, open to the external redox probe $[Fe(CN)_6]^{3-/4-}$, 10 mM, at pH < 4.5, when the polymer chains are protonated. At pH > 5.5, the interfacial electron-transfer process was effectively inhibited. As the polymer brush was deprotonated, the P4VP polymeric film collapsed, restricting access of the redox probe to the electrode surface. This pH-switchable polymer-brush-functionalized interface was then used to transduce pH changes, generated upon processing biochemical signals by the multienzyme logic system, into electronic signals (currents or electron transfer resistances), which were read out electrochemically from the modified electrode.

In order to demonstrate the possibility of processing multiple biochemical signals by enzyme logic systems, we designed a biocatalytic system performing a sequence of chemical reactions activated by four different chemical input signals: NADH (input A), acetaldehyde (input B), glucose (input C), and oxygen (input D) (Scheme 2A). The input signals were considered to be **0** in the absence of the respective chemicals (Ar was bubbled through the solution in order to remove O_2 when needed), while the input signals were **1** in the presence of the chemicals added at the selected concentrations. The operating concentrations of the chemical inputs were selected to produce substantial pH changes in an unbuffered solution (0.1 M in Na_2SO_4), as a result of biochemical reactions. Similarly to digitalization of signals used

(23) Carolus, M. D.; Bernasek, S. L.; Schwartz, J. *Langmuir* **2005**, *21*, 4236–4239.
(24) (a) Randles, J. E. B. *Discuss Faraday Soc.* **1947**, *1*, 11–19. (b) Ershler, B. V. *Discuss Faraday Soc.* **1947**, *1*, 269–277. (c) Bard, A. J.; Faulkner, L. R. *Electrochemical Methods: Fundamentals and Applications*; Wiley: New York, 1980.
(25) (a) Pita, M.; Katz, E. *Electroanalysis* **2008** (in press). (b) Tokarev, I.; Orlov, M.; Katz, E.; Minko, S. *J. Phys. Chem. B* **2007**, *111*, 12141–12145. (c) Katz, E.; Willner, B.; Willner, I. *Biosens. Bioelectron.* **1997**, *12*, 703–719.
(26) Motornov, M.; Sheparovych, R.; Katz, E.; Minko, S. *ACS Nano* **2008**, *2*, 41–52.

Scheme 1. Reversible Switching of Polymer-Brush-Modified Electrode between OFF and ON States upon Protonation/Deprotonation of Polyelectrolyte Chains

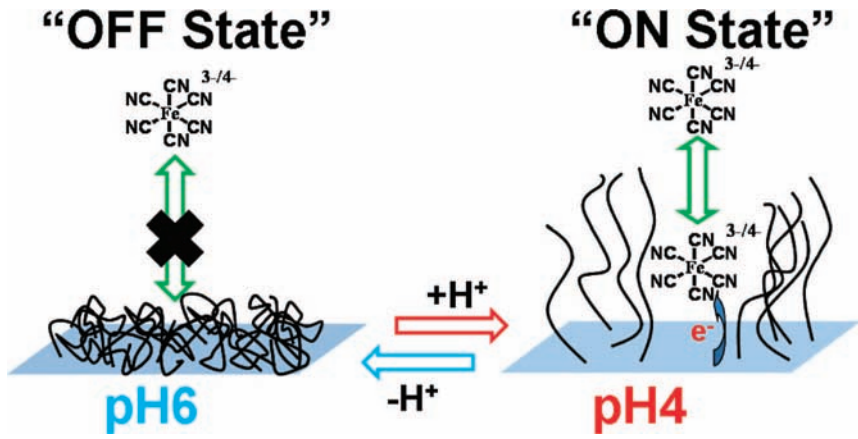

Scheme 2. (A) Biocatalytic Cascade Used for Logic Processing of Chemical Input Signals and Producing in Situ pH Changes as Output Signal. (B) Equivalent Logic Circuitry for Biocatalytic Cascade

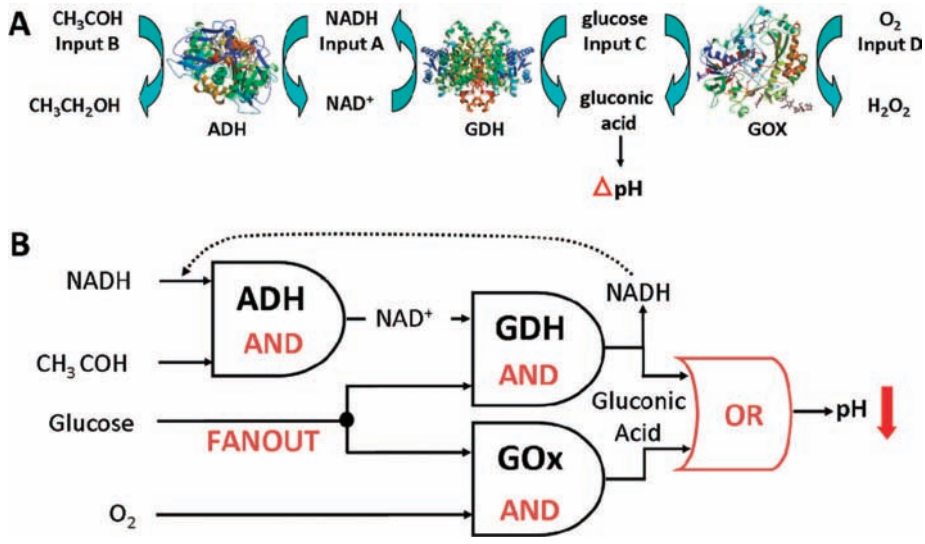

in electronics, we considered the intermediate values of the concentrations of the chemical inputs as undefined signals. It should be noted that only one of the biocatalytic reactions, the production of gluconic acid, resulted in pH changes, while all other reaction steps did not affect the pH value. The reaction resulting in the acidic pH was considered as the final output step of the biocatalytic cascade that controlled the interfacial properties of the modified electrode, thus allowing transduction of pH changes into electronic signals.

The biocatalytic cascade could be represented by equivalent logic circuitry (Scheme 2B). Indeed, the NAD^+ production biocatalyzed by ADH can be activated only in the presence of both input signals, NADH and acetaldehyde, thus realizing the AND logic gate, which is activated only by the **1**,**1** combination of the input signals. The next logic gate in the circuitry is composed of GDH and produces gluconic acid upon biocatalytic oxidation of glucose in the presence of NAD^+. Glucose is an independent input signal for this reaction, while NAD^+ is produced in situ as the result of the previous biocatalytic reaction (it is an output signal of the preceding AND logic gate). The oxidation of glucose is activated only in the presence of both inputs, glucose and NAD^+, thus again realizing the AND logic operation (activated only by **1**,**1** input signals). It should be noted that the byproduct of this reaction is NADH, which recycles to the input of the first AND logic gate (a feedback loop). Another logic gate composed of GOx, working in parallel with the first two AND gates, consumes glucose and oxygen to produce gluconic acid. Since the reaction biocatalyzed by GOx is activated only in the presence of both input signals, glucose and O_2, this reaction yields the AND logic gate as well (activated only by **1**,**1** input signals). Note that the glucose input signal is used by two parallel biochemical reactions (two parallel logic gates), involving the FANOUT function, which is trivial for electronics but requires consideration in biochemical systems. Finally, gluconic acid is produced in two parallel reactions, biocatalyzed by GDH and GOx. This results in lowering the pH value upon activation of either enzymatic pathway, thus mimicking the logic operation OR, which is activated by the **1**,**1** or **1**,**0** or **0**,**1** combination of the input signals.

The designed biocatalytic system, composed of three enzymes and activated by four chemical input signals, can operate differently upon application of the input signals in various combinations. Actually, the "correct" combination of the input signals resulting in the production of gluconic acid can be easily predicted on the basis of the sequence of biochemical reactions (Scheme 2A). We performed an experimental study of pH changes with time upon application of each of the 16 combinations of four input signals (Figure 1). The experiments were

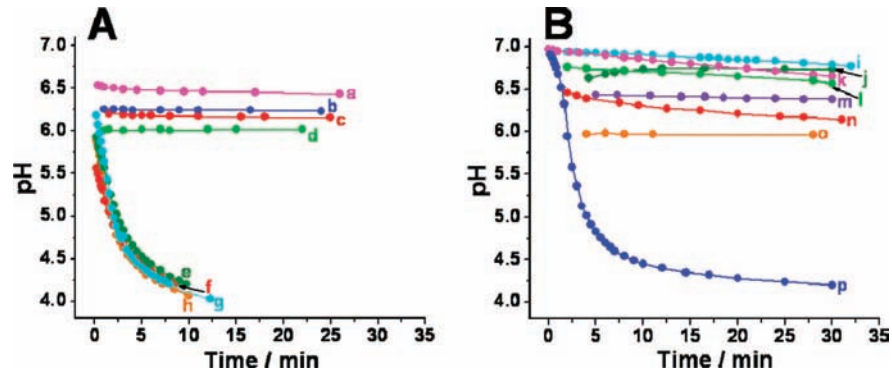

Figure 1. pH changes generated in situ by the enzyme logic network: (A) Variation of pH with time for oxygenated solutions upon application of various combinations of chemical input signals A−D: (a) **1**,**1**,**0**,**1**; (b) **1**,**0**,**0**,**1**; (c) **0**,**0**,**0**,**1**; (d) **0**,**1**,**0**,**1**; (e) **1**,**0**,**1**,**1**; (f) **0**,**1**,**1**,**1**; (g) **1**,**1**,**1**,**1**; and (h) **0**,**0**,**1**,**1**. (B) Variation of pH with time for deoxygenated solutions upon application of various combinations of chemical input signals A−D: (i) **0**,**0**,**1**,**0**; (j) **0**,**0**,**0**,**0**; (k) **0**,**1**,**1**,**0**; (l) **1**,**1**,**0**,**0**; (m) **1**,**0**,**0**,**0**; (n) **1**,**0**,**1**,**0**; (o) **0**,**1**,**0**,**0**; and (p) **1**,**1**,**1**,**0**. All solutions contained alcohol dehydrogenase (ADH), glucose dehydrogenase (GDH), and glucose oxidase (GOx), 10 units·mL^{-1} each, dissolved in 0.1 M Na_2SO_4. Input A was 0.5 mM NADH, input B was 5 mM acetaldehyde, input C was 12.5 mM glucose, and input D was dissolved oxygen in equilibrium with air.

Table 1. Truth Table for the Boolean Logic Function O = [(A AND B) AND C] OR (C AND D)[a]

input signal				output signal
A, NADH	B, acetaldehyde	C, glucose	D, O_2	O, decrease in pH (ΔpH > 2)
0	0	0	0	0
1	0	0	0	0
0	1	0	0	0
0	0	1	0	0
0	0	0	1	0
1	1	0	0	0
1	0	1	0	0
1	0	0	1	0
0	1	1	0	0
0	1	0	1	0
0	0	1	1	1
0	1	1	1	1
1	0	1	1	1
1	1	0	1	0
1	1	1	0	1
1	1	1	1	1

[a] O is the output signal and A−D are input signals. The chemical system was composed of three enzymes (glucose oxidase, glucose dehydrogenase, and alcohol dehydrogenase) performing four logic operations activated by four input signals.

always started at neutral pH values of ca. 6−7. Since the background solution was unbuffered, the initial pH values depended on the applied chemical inputs. Some of the input combinations did not result in the production of gluconic acid, thus keeping the original pH value unchanged. Input combinations that led to production of gluconic acid generated an acidic pH < 4.5 in ca. 5−8 min. The unchanged pH value was considered as the output signal **0**, while pH < 4.5 was considered as the output signal **1**. The results are summarized in Table 1, which is actually the truth table for the Boolean logic function characteristic of the logic network shown in Scheme 2B: O = [(A AND B) AND C] OR (C AND D), where O is the output, and A, B, C, and D are input signals. After the solution pH decreased as a result of the biocatalytic reactions producing output signal **1**, the initial pH value was reset by adding urease (2.5 units·mL^{-1}) and urea (2.5 mM).

pH changes in the solution were generated via two different pathways biocatalyzed by GOx and GDH, each activated by different combinations of the chemical input signals. In order to obtain comparable output signals (ΔpH) through each pathway, the kinetics of the two biocatalytic reactions should be balanced. This is a function of the FANOUT gate, when the same chemical input is fed into two (or more) chemical reactions. To tune the kinetics of our system, we followed changes of pH in the presence of different ratios of GOx and GDH (Figure 2). Relative amounts of gluconic acid generated by each pathway can be adjusted by varying the enzyme ratio on the basis of the kinetics of measured pH changes. For example, using GOx with activity of 1 unit·mL^{-1} and the ADH−GDH chain with activities of each enzyme of 10 units·mL^{-1} (Figure 2, curve c), the final pH value of 4.2 can be reached in half the time required when only the ADH−GDH pathway was used. This implies that the FANOUT gate feeds glucose into the two pathways in proportion that results in approximately equal output rate of the two catalytic branches.

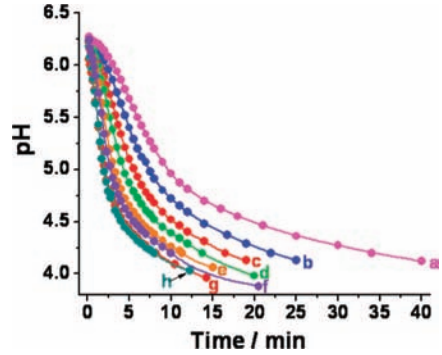

Figure 2. Variation of pH with time for the solutions with different ratios of GOx and GDH. All solutions contained 0.1 M Na_2SO_4 and inputs combination **1**,**1**,**1**,**1**. Input A was 0.5 mM NADH, input B was 5 mM acetaldehyde, input C was 12.5 mM glucose, and input D was dissolved oxygen in equilibrium with air. Activities of alcohol dehydrogenase (ADH) and glucose dehydrogenase (GDH) were kept constant at 10 units·mL^{-1} each. Activities of glucose oxidase (GOx) were (a) 0, (b) 0.5, (c) 1, (d) 2, (e) 3.5, (f) 5, (g) 7.5, and (h) 10 units·mL^{-1}.

One possible effect of the feedback loop (internal replenishment of NADH) present on the GDH side of our gate network may be that while the concentration of NADH corresponding to the logic value **1** was significantly smaller than that for all other inputs, it sufficed for the network to function for the duration of experiments, which in some cases lasted as long as 60 min. We point out that the main effect of feedback loops in network design is on the *time dependence* of the signal buildup. However, in our case the investigation was focused on the final signal values at large enough times, while the time dependence (Figures 1 and 2) showed no noteworthy features. Thus, the

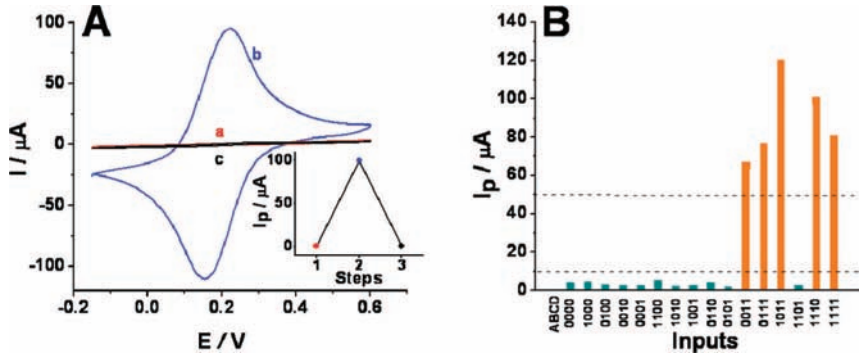

Figure 3. (A) Sample cyclic voltammograms obtained for the ITO electrode modified with the P4VP polymer brush in (a) the initial OFF state, pH ca. 6.7; (b) the ON state enabled by the input combination **1**,**1**,**1**,**0**, recorded at pH ca. 4.3; and (c) in situ reset to the OFF state, pH ca. 8.8. (Inset) Step 1, maximum current of the anodic feature recorded for the initial OFF state; step 2, anodic peak current for the ON state; step 3, maximum current of the anodic feature after a reset to the OFF state. Deoxygenated unbuffered solution of 0.1 M Na_2SO_4, 10 mM $K_3Fe(CN)_6$, and 10 mM $K_4Fe(CN)_6$ also contained ADH, GDH, and GOx, 10 units·mL^{-1} each. Input A was 0.5 mM NADH, input B was 5 mM acetaldehyde, and input C was 12.5 mM glucose. Potential scan rate was 100 mV·s^{-1}. (B) Anodic peak currents, I_p, for the 16 possible input combinations. Data were obtained from cyclic voltammograms recorded under the same conditions as in panel A. Dotted lines show threshold values separating logic **1**, undefined, and logic **0** output signals.

feedback loop on the GDH side does not introduce any delays, speedups, or instabilities in the present regime of the network operation. Therefore, our electrochemical results in what follows were obtained with the FANOUT (balancing of the GOx vs GDH sides of the gate functions) in the regime of activity of GOx, 10 units·mL^{-1}, which yielded *fast* gate functions. It should be noted that a low concentration of the NADH input signal also avoids the buffering properties this molecule possesses in the pH range used.

The initial pH value of ca. 6−7 corresponded to the OFF state of the P4VP-functionalized ITO electrode, while the acidic pH < 4.5 resulted in the ON state, when the interfacial redox process for the external redox probe $[Fe(CN)_6]^{3-/4-}$, 10 mM, was activated. This allowed transduction of the chemical output signal (ΔpH) into the electronically readable signal analyzed by cyclic voltammetry or impedance spectroscopy. Figure 3A shows typical cyclic voltammograms obtained at the P4VP-functionalized ITO electrode with different combinations of the chemical input signals applied in situ. The experiments were always started at pH ca. 6−7, when the interface is blocked by the shrunken polymer-brush film and the electrochemical process is inhibited. The resulting cyclic voltammogram showed no peaks and very low capacitance currents due to the hydrophobic nature of the interface (Figure 3A, curve a). Similar cyclic voltammograms were obtained for all combinations of the input signals that do not produce pH changes (output signal **0**) (Table 1).

If the biocatalytic reactions produced in situ pH changes yielding pH < 4.5 (output signal **1**), the polymer brush was swollen and the interface was open for the redox probe. This resulted in a reversible electrochemical process with high peak current values ($I_p = 99\ \mu A$) in the cyclic voltammogram (Figure 3A, curve b). Similar cyclic voltammograms were also obtained for all combinations of input signals that resulted in pH changes (output signal **1**) (Table 1). The biocatalytic reset process, restoring the initial neutral pH value of the solution, resulted in redox process inhibition. The cyclic voltammogram obtained after the reset function resembled the initial cyclic voltammogram characteristic of the OFF state of the electrode (Figure 3A, curve c). The stepwise activation and deactivation of the electrochemical process can be characterized by following the peak current values (I_p) in the cyclic voltammograms (Figure 3A, inset). The transition of the OFF electrode state, showing no peak currents in the cyclic voltammograms, to the ON state, with high peak currents, was achieved only when the logic output of the biochemical system was **1**.

The current responses derived from the cyclic voltammograms upon application of different combinations of chemical input signals are summarized in Figure 3B. Low currents ($I_p < 10\ \mu A$), obtained from the cyclic voltammograms for the OFF state of the interface, were considered as electronic output signal **0**, while high peak currents ($I_p > 50\ \mu A$), recorded for the ON state of the interface, were accepted as output signal **1**. It should be noted that cyclic voltammograms recorded in the OFF state and showing no redox process offered little useful information for the quantitative characterization of the "closed" interface. In order to obtain information about the OFF state, we applied Faradaic impedance spectroscopy,[27] which allows quantitative characterization of interfaces with high electron-transfer resistances.[28]

The impedance spectra were recorded upon application of each of the 16 combinations of chemical input signals, resulting in OFF and ON states of the modified electrode, similarly to the experiments with cyclic voltammetry. Figure 4A, curve a, shows a typical impedance spectrum in the form of a Nyquist plot obtained in the case when the applied chemical input signals did not result in a pH decrease (output signal **0**). The electrode was in the OFF state, showing large electron transfer resistance ($R_{et} = 86\ k\Omega$). The "successful" combination of input signals resulted in formation of gluconic acid, lowering the pH value and yielding the ON state of the interface with small electron transfer resistance ($R_{et} = 17\ k\Omega$) (Figure 4A, curve b). Subsequent application of the reset function raised the pH value and returned the interface to the OFF state. The corresponding impedance spectrum demonstrates high electron transfer resistance ($R_{et} = 92\ k\Omega$) similar to its original value (Figure 4A, curve c).

Reversible switching between the ON and OFF states can be characterized by the cyclic changes of R_{et} (Figure 4A, inset). The OFF states of the interface, characterized by high electron-transfer resistance, were obtained for all combinations of the input signals that do not change the pH value (output signal **0**),

(27) (a) Stoynov, Z. B.; Grafov, B. S.; Savova-Stoynova, B. S.; Elkin, V. V. *Electrochemical Impedance*; Nauka: Moscow, 1991. (b) *Impedance Spectroscopy: Theory, Experiment, and Applications*; Barsoukov, E., Macdonald, J. R., Eds.;Wiley-Interscience: Hoboken, NJ, 2005.
(28) Katz, E.; Willner, I. *Electroanalysis* **2003**, *15*, 913–947.

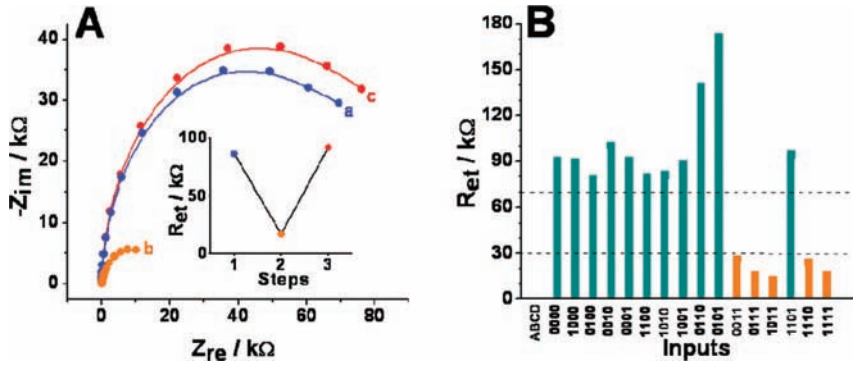

Figure 4. (A) Sample impedance spectra (in the form of Nyquist plots) for (a) the initial OFF state, pH ca. 6.5; (b) the ON state enabled with the input combination **1**,**1**,**1**,**1**, recorded at pH ca. 4.0; and (c) in situ reset to the OFF state, pH ca. 8.8. (Inset) Step 1, R_{et} of the initial OFF state; step 2, R_{et} for the ON state; step 3, R_{et} for reset to the OFF state. Unbuffered solution of 0.1 M Na_2SO_4, 10 mM $K_3Fe(CN)_6$, and 10 mM $K_4Fe(CN)_6$ also contained ADH, GDH, and GOx, 10 units·mL^{-1} each. Input A was 0.5 mM NADH, input B was 5 mM acetaldehyde, input C was 12.5 mM glucose, and input D was dissolved oxygen in equilibrium with air. (B) Electron transfer resistance, R_{et}, for the 16 possible input combinations. Data were derived from impedance spectra obtained under the same conditions as in panel A. Dotted lines show threshold values separating logic **1**, undefined, and logic **0** output signals.

while the "successful" combinations resulted in an acidic medium (output signal **1**), producing the ON state characterized by low values of R_{et} (Figure 4B). Electronic output signals derived from the impedance spectra were determined as **0** when the electron transfer resistance is large ($R_{et} > 70$ kΩ) and as **1** when the electron transfer resistance is small ($R_{et} < 30$ kΩ). It should be noted that electronic output signals in the form of peak currents, I_p, and in the form of electron transfer resistances, R_{et}, were the same in the logical form (**0** or **1**) for similar combinations of input signals regardless of the applied electrochemical method. Electronic output signals in the form of **0** or **1** also correlated with the logic values of the ΔpH output signals summarized in Table 1.

Chemical input signals were applied at their zero concentrations (considered as logic **0** value) and at high concentrations (defined as logic **1** value). Global mapping of the logic gate transduction function upon application of variable concentrations of all chemical input signals, to optimize the gate performance function,[16] was outside the scope of the present study. Nonetheless, we elected to vary the glucose concentration while keeping all other chemical input signals at their logic value **1** and analyze the electronic signal output in the form of peak currents derived from the cyclic voltammograms. This mapping of the network response is of particular interest because for the realized Boolean logic, it is the only input combination that results in signal variation between two Boolean values in response to varying a *single* input (glucose).

Prior to the response-mapping experiment, we titrated the background solution (0.1 M in Na_2SO_4) to different pH values by adding small volumes of 0.1 M H_2SO_4, starting from neutral pH values, when the electrode is in the OFF state, and moving to a sufficiently acidic pH range to activate the electrochemical process. The titration curve, showing the peak current values as a function of solution pH, demonstrates the transition of the electrode from the OFF state to the ON state upon acidification of the solution (Figure 5, curve a). The data were nicely fitted with a hyperbolic tangent sigmoid curve, $0.50-0.50 \times \tanh[(W - 4.85)/0.36]$, where W is pH.

Next, we performed a "titration" of the system with different concentrations of glucose. Prior to recording cyclic voltammograms, the biocatalytic reactions were carried out for 20 min at each concentration of glucose. The resulting peak currents were plotted as a function of the glucose concentration (Figure 5, curve b). The curve was drawn though the data points with the

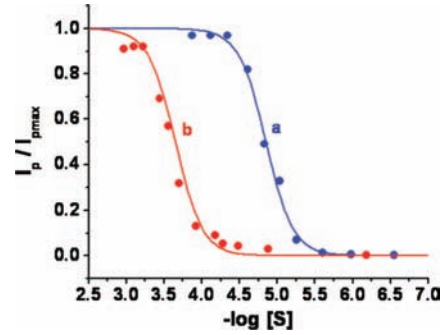

Figure 5. Output signal, represented by anodic peak current rescaled to the dimensionless "logic variable" range from **0** to **1**, plotted as a function of −log [S]. (Curve a) $S = H^+$; the pH was changed by titrating a solution with input combination A, B, C, D = **0**,**0**,**0**,**1**, with 0.1 M H_2SO_4; cyclic voltammograms were recorded after 10 min was allowed for the working electrode to equilibrate at each pH. (Curve b) S = glucose; pH changes generated in situ by biocatalytic reactions with input combination **1**,**1**,**1**,**1**, where concentrations of glucose ranged from 6.7×10^{-7} to 1.1×10^{-3} M. Unbuffered solution of 0.1 M Na_2SO_4, 10 mM $K_3Fe(CN)_6$, and 10 mM $K_4Fe(CN)_6$ also contained ADH, GDH, and GOx, 10 units·mL^{-1} each. Input A was 0.5 mM NADH, input B was 5 mM acetaldehyde, input C was glucose with variable concentrations, and input D was dissolved oxygen in equilibrium with air.

same slope at inflection as for the acid titration: $0.50-0.50 \times \tanh[(W - 3.65)/0.36]$, where W is −log [glucose] (in molar units). It is interesting that the function resembles the titration curve with a typical sigmoid shape, demonstrating a sharp transition from the OFF state to the ON state of the electrode in the range of glucose concentrations between ca. 0.15 and 0.4 mM.

It should be noted that chemical/biochemical systems usually produce an approximately linear, typically convex response function of the concentrations (sometimes reaching saturation, as in the case of Michaelis−Menten kinetics for enzymatic reactions). The convex response function, when it is applied to Boolean logic operations, results in an amplification of analog noise level for at least one of the **0** and **1** logic values.[16] The response function obtained in the present system resembles the sigmoid functions of electronic filters and results in the suppression of analog noise level at digital **0** and **1** values of the input signal. The sigmoid response function originates not from the chemical kinetics of the enzyme-catalyzed reactions but rather from the response of the polymer brush at the electrode surface. Thus, a similar sigmoid shape (noise-

suppression property) might be expected also for all other chemical input signals since all of them are coupled with the electronic output signal via in situ titration of the polymer brush at the electrode surface.

Conclusions and Perspectives

The studied system demonstrated the possibility to process complex patterns of biochemical signals, processing information by enzyme reactions. Stable information processing with clearly distinguishable output signals from various multiple-input combinations of biochemical signals was achieved. The studied enzymatic logic system has several interesting features resulting in a new step in the development of enzyme logic networks. A four-input biochemical logic network has been realized, where the output signal is read out electronically by coupling biocatalyzed reactions to a pH-sensitive polymer-brush-functionalized electrode. The network is rich enough to contain four conventional gates (AND and OR) but also involves a signal splitting (for glucose): the FANOUT "gate". In addition to carrying out the AND gate, the enzyme glucose dehydrogenase (GDH) also produces NADH that is the input for the function of the enzyme alcohol dehydrogenase (ADH), which carries out the preceding AND gate in the network. Thus, this scheme also involves a feedback loop, though in our regime of operation the network showed no special feature as a result. When the pH drop is transduced into an electric signal at the electrode, the latter demonstrates a "filtering" effect: a "sigmoid" processing of the signal that significantly suppresses errors.

Coupling of a multicomponent/multisignal-responsive enzyme logic network with a sensing electrode allows electronic transduction of the chemical signals processed by the system into electronic outputs in the form of currents or interfacial resistances. This signal-transducing interface could be applied in various "smart" bioelectronic devices ranging from biosensors[18,19] to biofuel cells[20] controlled by in situ biochemical/physiological conditions.

The difference of the presently studied system from previously designed enzyme logic gates is the complexity of its composition and sophistication of the information processing. This is the next step toward the ultimate goal of using natural biochemical pathways to directly control implantable bioelectronic devices. Additional important steps waiting to be studied are as follows: (i) Further increase of the enzyme logic complexity is needed for future integration of biomedical devices with natural in vivo biochemical pathways. (ii) Enzyme systems processing biochemical signals should be directly immobilized on the signal-transducing interfaces. (iii) Noise reduction in signal processing should be studied, and the role of the sigmoid shape of the transducing function in noise suppression should be further addressed. This will be particularly important for the development of future robust information-processing and actuating bioelectronic devices. (iv) Different mechanisms for the coupling between signal-processing biochemical systems and signal-transducing electronic interfaces should be studied. The present system is based on proton exchange between the biochemical system and the sensing interface. Other mechanisms might be based on electron exchange with the use of redox-active polymers immobilized at the sensing interface. (v) The present information-processing enzyme system serves merely as an example of a sophisticated information-processing pathway and has no biomedical meaning. The next step should include the design of an enzyme system processing biochemical information with the use of important physiological markers as input signals at their natural concentrations. Analysis of their specific concentration patterns will allow autonomous operation of medical bioelectronic devices controlled by the patient body and performing operations (e.g., signaling or drug delivery) on demand. Potential candidates for these biomedical markers could be lactate,[29] glucose,[30] and norepinephrine,[31] signaling different kinds of injuries.

Although there are still many scientific and technological challenges to be overcome, we anticipate that such enzyme logic networks responding to complex patterns of biomarkers and coupled with electronic transducers and actuators will revolutionize medical treatment, particularly in cases of emergency.

Acknowledgment. This research was supported by the NSF Grant "Signal-Responsive Hybrid Biomaterials with Built-in Boolean Logic" (DMR-0706209). An award from the Semiconductor Research Corporation: "Cross-disciplinary Semiconductor Research" (2008-RJ-1839G) is gratefully acknowledged. M. Privman acknowledges the award of a faculty development fellowship by Empire State College for a reassignment to carry out this research project. T.K.T. acknowledges a Wallace H. Coulter scholarship from Clarkson University.

JA8088108

(29) Kline, J. A.; Maiorano, P. C.; Schroeder, J. D.; Grattan, R. M.; Varyl, T. C.; Watts, J. A. *J. Mol. Cell. Cardiol.* **1997**, *29*, 2465–2474.
(30) Zink, B. J.; Schultz, C. H.; Wang, X.; Mertz, M.; Stern, S. A.; Betz, A. L. *Brain Res.* **1999**, *837*, 1–7.
(31) (a) Rosenberg, J. C.; Lillehei, R. C.; Longerbeam, J. L.; Zimmermann, B. *Ann. Surg.* **1961**, *154*, 611–627. (b) Prasad, M. R.; Ramaiah, C.; McIntosh, T. K.; Dempsey, R. J.; Hipkeos, S.; Yurek, D. *J. Neurochem.* **1994**, *63*, 1086–1094.